

Effectiveness Analysis of Infinite Impulse Response Digital Filter on Electrocardiogram Signal to Extract Respiration Rate Signal



Halida Hasrifah, Muhammad Ridha Mak'ruf, Andjar Pudji,
Levana Forra Wakidi, Bambang Guruh Irianto, Triwiyanto,
and Anilkumar Suthar

Abstract Respiration Rate (RR) is the number of respirations or movements that determine inspiration and expiration calculated in breaths per minute (BrPM). The Respiration Rate Signal can be extracted from an electrocardiogram signal (ECG-Derived Respiration). There have been many studies to extract the respiration rate signal from the ECG signal but there has been no study on the effectiveness of extracting the respiration rate signal with a digital filter, therefore, this study aimed to determine the effectiveness of the Infinite Impulse Response (IIR) digital filter in the design of the Butterworth Filter and the Chebyshev I filter based on the selection of different orders, namely orders 4, 6, and 8 to extract the Lead II Electrocardiogram signal-based Respiration Rate signal. This study used the AD8232 ECG module, Arduino Nano, Ms. Excel, and MATLAB. The method used to analyze the signal was the Fast Fourier Transform (FFT) method. The tricks were to determine the components of the mean frequency, the mean power frequency, and the mean power frequency respiration rate obtained from the use of the IIR digital filter on respondents which would be compared with the gold standard in the form of phantom. The results were analyzed using a correlation analysis where in the Butterworth filter, the highest correlation value is 0.996 in order 6 while in the Chebyshev I filter, the highest correlation value is 0.999 in order 8. It can be concluded that the Chebyshev I digital filter of order 8 has the best effectiveness value.

Keywords Electrocardiogram · Infinite impulse response · AD8232 · Respiration rate

H. Hasrifah · M. R. Mak'ruf (✉) · A. Pudji · L. F. Wakidi · B. G. Irianto · Triwiyanto
Department of Medical Electronics Technology, Poltekkes Kemenkes Surabaya, Surabaya,
Indonesia
e-mail: ridha@poltekkesdepkes-sby.ac.id

A. Suthar
New LJ Institute of Engineering and Technology, Gujarat Technological University, S.G.
Highway, Ahmedabad, Gujarat, India

© The Author(s), under exclusive license to Springer Nature Singapore Pte Ltd. 2023
T. Triwiyanto et al. (eds.), *Proceeding of the 3rd International Conference on Electronics, Biomedical Engineering, and Health Informatics*, Lecture Notes in Electrical Engineering 1008, https://doi.org/10.1007/978-981-99-0248-4_41

1 Introduction

Carbon dioxide and oxygen are exchanged in the body during respiration, a crucial physiological activity [1, 2]. Respiration Rate (RR) is the number of respirations or movements that determine inspiration and expiration calculated in breaths per minute (BrPM) [3, 4]. Normal breathing for adults is in the range of 12–20 times per minute [5], if there is a condition of $RR > 27$ then it indicates abnormalities in the heart system [6, 7]. Chronic obstructive pulmonary disease (COPD), congestive heart failure (CHF), and abnormal respiratory waveforms are a few disorders that can be detected early using respiration rate [6, 8–10].

The respiration rate signal can be obtained from the extraction of ECG or PPG signal [4, 11–15]. Signal extraction from ECG is called the ECG-derived respiration (EDR) technique. This EDR technique utilizes from single lead (Lead II) ECG signal leads by using gel electrodes when mounting on subjects [6, 10, 16, 17]. In this study, the focus was on extracting the respiration rate signal from the ECG signal (EDR) by utilizing the filter process. The filter functions to pass the cool signal frequencies and withstand unwanted signal frequencies. In the process of extracting, the filter signal used can be analog filters or digital filters. In analog filters, there is a disadvantage, namely, there is still much noise during the filtering process of the respiration rate signal from the ECG signal. Whereas, in digital filters, the noise produced is not as much as in analog filters [18, 19]. Digital filters are better in the use of the process of decreasing the signal respiration rate of the ECG, and in terms of the level of accuracy and precision, digital filters are more accurate and precise.

Heman Sharma, et al., in 2015, conducted a study on respiration rate signal subduction from a single lead ECG using homomorphic filtering methods (discrete Fourier transform (DFT) and discrete cosine transform (DCT)) with a frequency from 0.2 to 0.8 Hz. The results obtained based on the Kaiser window on the extraction of respiration rate signal showed that the use of the Butterworth filter was better than those of the Chebyshev I and FIR filters. This study still needs to be continued to carry out further analysis regarding the selection of filters and orders in the extraction of respiration rate signal [20].

Next, Preeti Jagadev, et al., in 2019 [21], conducted a study by using thermal cameras to monitor respiration rate with the algorithm method of Ensemble of regression trees, which is a method of comparing the performance of several IIR digital filters and an FIR filter. The results obtained showed that the extraction of respiration rate using the Butterworth filter was better, and the filter performance is good every time there is an increase in the filter order. A study by Christna Orphannidou in 2016, used the algorithm method of EEMD in IMF2 and IMF3 to retrieve EDR/PDR signal. An FIR filter was set on a band pass filter with a frequency from 0.1 to 0.6 Hz. The results obtained showed that the performance of the ECG was better than the PPG, although there was no significant difference. Respiration rate showed a mean absolute error of 1.8 bpm and a mean average error of 10% [4]. A study by Subhadeep Basu, et al., in 2020, compared the Butterworth digital filter with the Chebyshev I filter to

see the effect of orders and cut off frequency on the ECG signal [18]. However, these filters have not been applied to analyze the respiration rate signal.

Based on the previous studies, the researchers of this study were interested in conducting a study on ECG-free respiration rate signal extraction using the Infinite Impulse Response (IIR) digital filter in the design of the Butterworth filter and the Chebyshev I filter in orders 4, 6, and 8 with the Baseline Wander method using a Band Pass Filter with a Cut Off frequency from 0.1 to 0.5 Hz, based on the frequency of respiration rate signal [22]. The data would be processed on a personal computer using MATLAB software and analyzed using frequency-based features such as mean frequency and mean power, and median frequency of the signal. This study aimed to investigate the IIR filter performance to extract the EDR signal.

2 Material and Methods

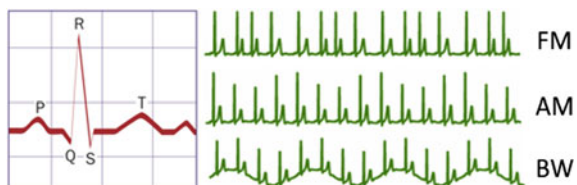
2.1 Theoretical Background

ECG-derived respiration. ECG-derived respiration (EDR) is an ECG-based respiration rate signal extraction technique and is a non-invasive method for monitoring respiratory activity when the respiration rate signal is not recorded [16, 20]. In the clinical world, this method provides convenience because it allows for simultaneous monitoring of cardiac and respiratory signals from the ECG signal that has been recorded. The EDR technique has a category of methods, namely the multiple lead method based on the Angle of Mean Electrical Axis variation, the single lead method based on the R-wave amplitude (AM) frequency modulation (FM), and the baseline wander (BW), in addition to the heart rate-based method, discrete wavelet transform method, and band pass filter method [9, 22–25].

Of the several categories of methods used by the EDR technique above, the researchers applied the single lead method based on the baseline wander (BW) [2, 11, 12]. This baseline wander method uses a band pass filter with a cut off frequency from 0.1 to 0.5 Hz [10, 22, 23]. The following Fig. 1 shows the ECG-Derived Respiration (EDR).

Figure 1 shows the Approach to the Baseline Wander method as a way to obtain a respiration rate signal from an ECG (EDR) signal. Baseline wander is when expansion and contraction of the chest cavity occur in the breathing process, resulting in the

Fig. 1 ECG-derived respiration (EDR)



movement of the electrodes relative to the heart that will cause baseline wander on the ECG signal [15, 26, 27].

Electrocardiogram Leads. Leads using 3 electrodes are commonly used for simple monitoring, while leads using 2 electrodes are for active monitoring. The Lead II configuration can be obtained by placing the electrodes using the Einthoven triangle system, namely, the electrodes are placed at the torso, namely the Right arm (RA), Right Leg (RL), and Left Leg (LL) [26, 28, 29].

Filter Infinite Impulse Response. Digital filters of a certain type, such as the infinite impulse response (IIR) filter, are employed in DSP applications. The benefit of using IIR filters is that they demand less efficiency for steep frequency response, which cuts down on the amount of processing time [30]. Therefore, a digital filter is needed to extract the respiration rate signal based on the ECG signal from the IIR filter design type, namely the Butterworth filter (BF) and the Chebyshev type I filter (CT1F). The following Eqs. 1 and 2 show the formula for BF and CT1F [21]:

$$y(n) = b_0x(n) + b_1x(n - 1) + \dots + b_Mx(n - M) - a_1y(n - 1) - \dots - a_Ny(n - N) \tag{1}$$

And, the IIR filter transfer function given is

$$H(z) = \frac{Y(z)}{X(z)} = \frac{b_0 + b_1z^{-1} + \dots + b_Mz^{-M}}{1 + a_1z^{-1} + \dots + a_Nz^{-N}} \tag{2}$$

where the M numerator and N denominator coefficients, respectively, are b_i and a_i . The z -transform functions of the filter input $x(n)$ and filter output $y(n)$ are $Y(z)$ and $X(z)$, respectively.

$$|H_n(j\omega)| = \frac{1}{\sqrt{1 + E^2\left(\frac{\omega}{\omega_c}\right)^{2n}}} \tag{3}$$

where, n is the filter order, ω is the angular frequency, ω_c is the cut off angular frequency, and E is the maximum band pass gain. The CT1F filter transfer function given is

$$|H_n(j\omega)| = \frac{1}{\sqrt{1 + R_f^2 T_n^2\left(\frac{\omega}{\omega_c}\right)}} \tag{4}$$

where, R_f is the ripple factor, and T_n is the Chebyshev polynomial of order n .

Fast Fourier Transform. In the sectors of education, business, and the military, the Fast Fourier Transform (FFT) is a crucial method for solving all sorts of issues.

This technique was first introduced by Gauss in 1805. However, FFT received attention during a seminar by Cooley and Tukey in 1965, where they found the main disciplines of digital signal processing [31]. The Fast Fourier Transform (FFT) transforms an analog time-domain signal into various frequencies using a complex exponential function [27]. Fast Fourier Transform can be defined by the following Eq. 5.

$$\begin{aligned}
 S(f) &= \int_{-\infty}^{\infty} s(t)e^{-j2\pi ft} dt \\
 S(f) &= \int_{-\infty}^{\infty} s(t) \cos(2\pi ft)dt - j \int_{-\infty}^{\infty} s(t) \sin(2\pi ft)dt \tag{5}
 \end{aligned}$$

where, $S(f)$ is a signal in the frequency domain, $s(t)$ is a signal in the time domain, and $s(t)e^{-j2\pi ft} dt$ is the signal value constant.

Fast Fourier Transform has an effective algorithm for computing Discrete Fourier Transform (DFT). The time it takes to evaluate the DFT on a computer mainly depends on the number of multiplications involved. DFT requires N^2 multiplication. FFT only takes $N\log_2(N)$. This algorithm’s fundamental idea is the understanding that a discrete Fourier transform of a series of N points can be represented in two discrete Fourier transforms of length $N/2$. So, if N is a power of two, it is possible to apply this decomposition recursively until a Discrete Fourier Transform of single point is obtained.

In digital signal processing (DSP) software, there are three classes of FFT commonly used, namely Decimation in Time (DIT), Decimation in Frequency (DIF) and Split Radix. Another type of FFT that has been used is parallel FFT uses parallel computing to sequence data so that the transformation process will be faster. FFT has a resolution of f_s/N where f_s is the value of the sampling rate and N is the number of sampled data. With computer limitations, the above equation, especially for the real part, can be approximated by the following Eq. 6.

$$\begin{aligned}
 \int_{-\infty}^{\infty} s(t) \cos(2\pi ft)dt &\rightarrow \sum_n x(n\Delta t) \cos(2\pi fn\Delta t)\Delta t \\
 &= \sum_n x(n\Delta t) \cos(2\pi nm\Delta t\Delta f)\Delta t \\
 &= \sum_n x(n\Delta t) \cos(2\pi \frac{nm}{N})\Delta t \tag{6}
 \end{aligned}$$

where, m and n are integers, in the time domain, the signal is defined as $T = N\Delta t$, while in the frequency domain, $\Delta f = \frac{f_s}{N}$ where Δf is the value of interval between frequency and $f_s = \frac{1}{\Delta t} = N\Delta f$. Thus, the equation $\Delta t\Delta f = \frac{1}{N}$ is the link between the time domain and the frequency domain. If the number of data N is smaller than the sampling frequency, the resulting frequency will not be precise. The sampling

frequency value must be greater than or equal to 2 times the maximum frequency value to avoid frequency aliasing [31].

Power Spectrum Density (PSD). The power present in a signal as a function of frequency is described by its power spectral density (PSD). When the signal is described just in voltage and there is no specific power connected with the amplitude, a PSD is typically stated in watts per Hertz (W/Hz). In this case, “power” is only considered in terms of the square of the signal, as its value will always be proportional to the actual power delivered by that signal within a given impedance. So, one can use the units $V^2 \text{ Hz}^{-1}$ for PSD and $V^2s \text{ Hz}^{-1}$ for ESD (Energy Spectrum Density) even though no power or energy is defined. Signal power intensity in the frequency domain is measured by a power spectral density, or PSD. The FFT spectrum of a signal is used to calculate a PSD. The amplitude and frequency content of a random signal can be characterized using information from a PSD [32]. A PSD can be defined using the following Eq. 7.

$$S_{xx}(\omega) = \lim_{\tau \rightarrow \infty} E \frac{[|\widehat{x}_T(\omega)|^2]}{\tau} \quad (7)$$

where, $S_{xx}(\omega)$ is the result of a power spectral density, $\widehat{x}_T(\omega)$ is the fast fourier transform of the Respiration Rate signal.

Frequency Domain Feature. Power Spectral Density is commonly used to extract the frequency domain information (PSD). Welch is employed in this study to calculate the power spectral density. The frequency domain features employed are represented by the mathematical Eqs. (8), (9), and (10).

Mean Frequency. The mean frequency is the average (mean) frequency calculated as the sum of the power spectrum products of the Respiration Rate signal and the frequency divided by the total number of spectrum intensities. The mean frequency defined using the following Eq. 8.

$$\text{MNF} = \frac{\sum_{j=1}^M f_j P_j}{\sum_{j=1}^M P_j} \quad (8)$$

where, f_j is the spectrum frequency, P_j is the power of the Respiration Rate signal, and M is the length of the signal frequency.

Median Frequency. The median frequency is the frequency at which the spectrum is divided into two regions of equal amplitude. The median frequency can be defined using the following Eq. 9.

$$\sum_{j=1}^{\text{MDF}} P_j = \sum_{j=\text{MDF}}^M P_j = \frac{1}{2} \sum_{j=1}^M P_j \quad (9)$$

where, MDF is the median frequency value, P_j is the power of the Respiration Rate signal, and M is the length of the Respiration Rate signal.

Mean Power. The Mean Power (MNP) is the average (mean) value of the power spectrum of the Respiration Rate signal, defined by the following Eq. 10.

$$\text{MNP} = \sum_{j=1}^M P_j / M \quad (10)$$

where, MNP is the mean power value, P_j is the power of the Respiration Rate signal, and M is the length of the Respiration Rate signal.

2.2 Data Set

This study was carried out by taking data on the phantom as a gold standard signal, data retrieval on the phantom was carried out with settings of 15, 20, and 30 brpm and heart settings of 80, 90, and 100 bpm, in each respiration rate setting with 10 recordings of each setting. The amount of data obtained from the recording of phantom signal was 90 data, the time required was approximately 2 h. Then, data on 10 respondents with an age range of 20–30 years for 10 times per respondent was taken. Respondents were positioned to sleep on their backs with a relaxed state without speaking, gel electrodes were placed in the Lead II ECG position on the chest, namely RA, RL, and LL [6, 26, 28, 29]. Figure 2 shows how data were taken on the phantom and respondents.

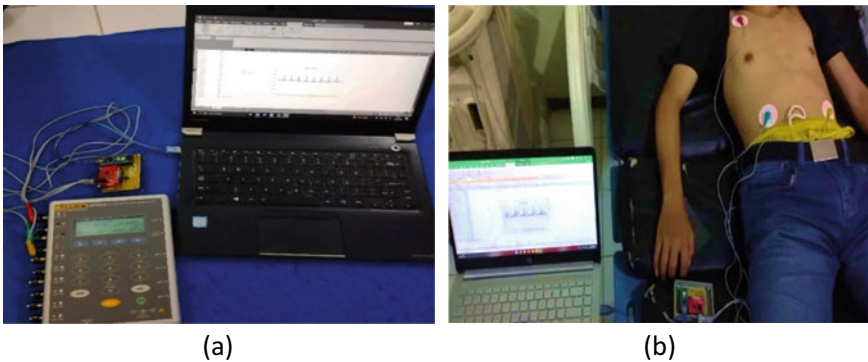


Fig. 2 Data collection **a** phantom **b** respondent

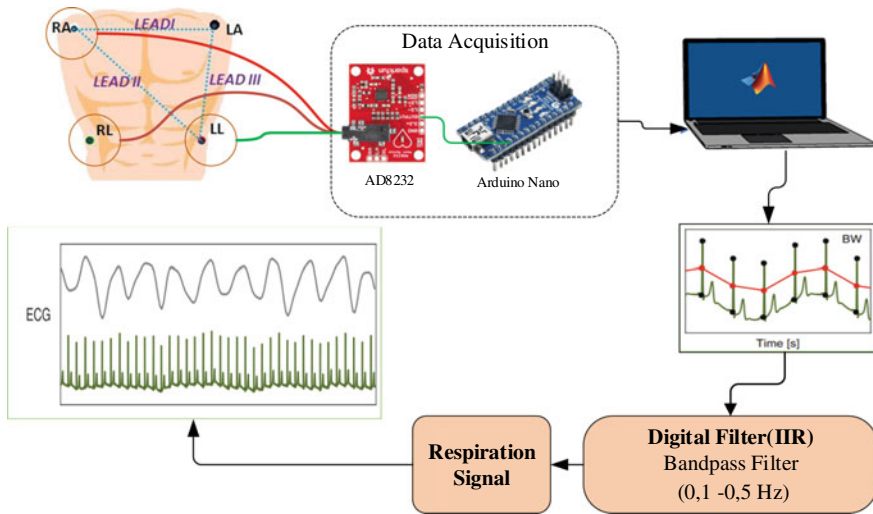


Fig. 3 Flowchart of experimental procedure

2.3 Experimental Procedure

This study used the AD8232 ECG Module to generate an ECG signal, Arduino Nano to be used as a microcontroller, MS. Excel to be used for signal recording, and MATLAB to be used for signal data processing [27, 33].

Figure 3 shows the research flowchart, where the output of the signal recorder by the AD8232 ECG Module is in the form of an ECG signal in the form of analog data that were processed on the Arduino. Arduino was used in this study as a microcontroller to forward the ANALOG ECG signal to a computer or PC to be displayed, recorded, and stored on MS. Excel. The stored analog signal was then be processed using MATLAB to extract the respiration rate signal based on the ECG signal using the Infinite Impulse Response (IIR) digital filter in the design of the Butterworth filter and the Chebyshev I filter in orders 4, 6 and 8.

2.4 Data Processing

Figure 4 shows the research framework, where the AD8232 ECG module output generates a lead II ECG signal. The ECG signal was recorded on MS. Excel with a sampling frequency of 100 Hz. Furthermore, the ECG signal was then processed in MATLAB software to go through the extraction process of the respiration rate signal.

The extraction process of the respiration rate of the ECG signal used the FFT method. This method will look at the frequency component of the ECG signal. After

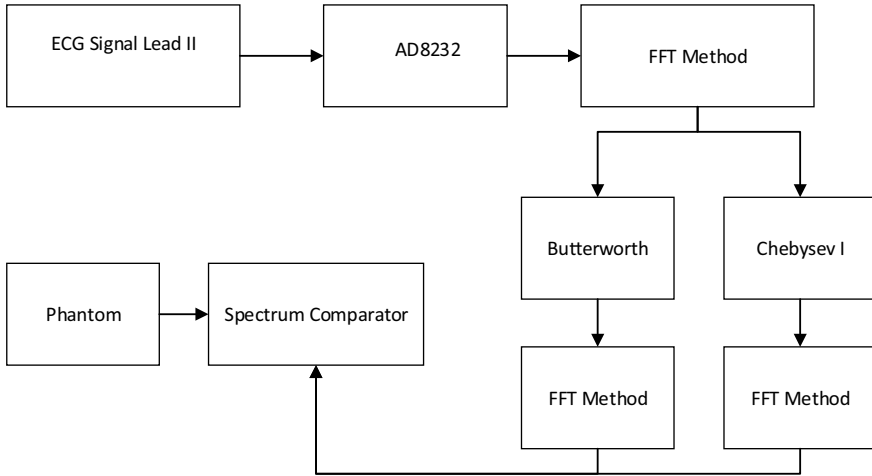


Fig. 4 Research framework

extracting the respiration rate, the signal was filtered using the IIR digital filter in the design of the Butterworth filter in orders 4, 6, 8 and the Chebyshev I filter in orders 4, 6 and 8. The signal that has been processed using the filters was then be reanalyzed by the frequency component using the FFT method. Furthermore, the results from the FFT analysis were processed using a spectrum comparator to see the effectiveness of the filters in extracting the respiration rate signal from the ECG. The effectiveness analysis process was carried out by comparing the shape and components of the respiration rate signal from the Butterworth filter and the Chebyshev I filter with the reference respiration rate signal derived from the phantom using a spectrum comparator.

2.5 Data Analysis

Mean. The calculation of the mean value is carried out to determine the trend of the heart rate measurement value and the respiration rate on the drowsiness level. The following Eq. 10 shows the mean value formula to be used in the data analysis process. In this equation, \bar{x} is the mean data, $\sum x_n$ is the data value, and n is the total data.

$$\text{mean}(\bar{x}) = \sum \frac{x_n}{n} \tag{11}$$

Relative Error. The relative error is used to determine the level of accuracy of the sensor reading to the actual value. The formula for the percent error or relative can be defined in the following Eq. 11.

$$\varepsilon_e = \frac{x_n - \bar{x}}{x_n} \times 100\% \quad (12)$$

where, X_n is the standard mean and \bar{X} is the research module mean.

Correlation. A correlation is intended to explore the degree of relationship between two variables. A correlation coefficient is the measure for determining the degree of relationship between variables. The correlation coefficient can be defined using the following mathematical Eq. 13.

$$R = \frac{n(\sum XY) - (\sum x) \cdot (\sum y)}{\sqrt{n \sum x^2 - (\sum x)^2 \cdot n(\sum y^2) - (\sum y)^2}} \quad (13)$$

where, n is the sum of the observations, x is the measurement of variable 1, y is the measurement of variable 2, $\sum xy$ is the sum of both variables, $\sum x$ is the sum of variable 1, $\sum y$ is the sum of variable 2, $\sum x^2$ is the sum of the squared values of variable 1, and $\sum y^2$ is the sum of the squared values of variable 2.

3 Results

3.1 Module Test Result

The results of the tool making are presented in Fig. 5, namely the front of the tool and the inside of the tool consisting of the AD8232 ECG Module and Arduino Nano. The ECG module used in this study is the type of “Fully integrated single-lead ECG front end” AD8232. The circuit of the AD8232 module has 3 inputs that can later be utilized for input from the electrodes. The 3-electrode configuration used is designed to monitor ECG waveform which operates at a voltage of 2.0–3.5 V. The Arduino Nano is a small, complete, and breadboard-friendly board based on the ATmega328 (Arduino Nano 3.x). It lacks only a DC power jack and works with a Mini-B USB cable instead of a standard one. An ADC (Analog to Digital Converter) is a type of analog-to-digital converter that converts a continuous analog waveform into a digital representation. The ADC pins on the Arduino Nano are 8 pins used in the study, namely the analog pin A4, the input voltage used is between 7 and 12 V, and the maximum current is 40 mA [33].

Figure 6 shows the sensor output in the form of an ECG signal displayed on the Digital Oscilloscope with a Time/DIV setting of 500 ms and Volt/DIV of 100 mv, so a sensor output amplitude of 120 mV is obtained. Figure 7 shows the testing of sampling frequency to determine the size of the Arduino sampling frequency. Testing is important, considering that the data from this testing are needed in the filter design process that will be used on the tool. To find out the sampling frequency, the researchers used the ADC reading program using analog pins and DigitalWrite

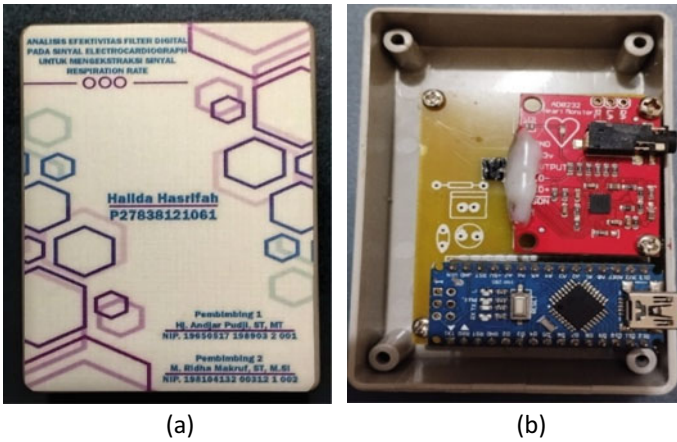


Fig. 5 a Module b inside of module

on the digital pin as output which will be measured by a digital oscilloscope with a Time/DIV setting of 5 ms and Volt/DIV of 2 V, so an Arduino sampling frequency of 100.148 Hz is obtained.

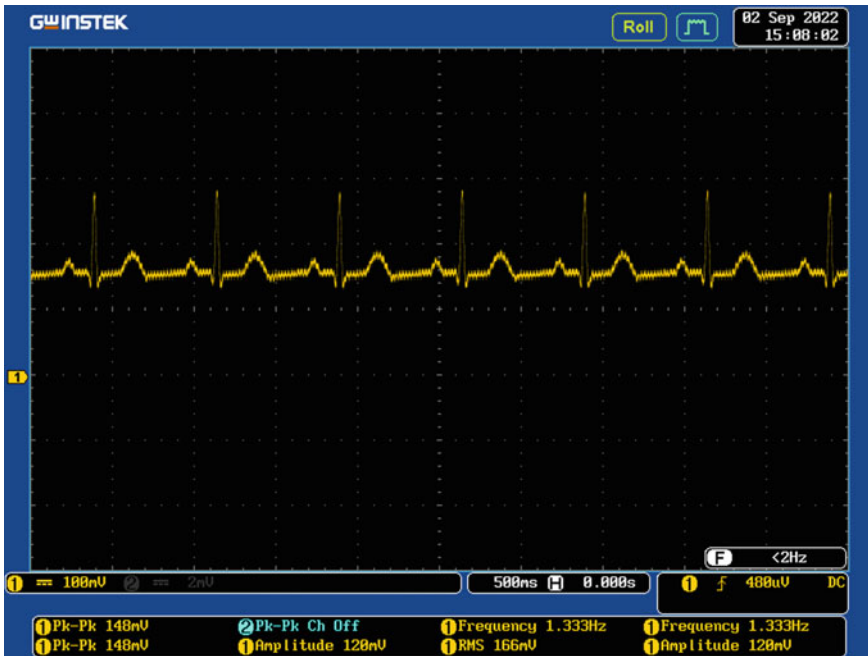


Fig. 6 Output of AD8232 ECG module on the oscilloscope

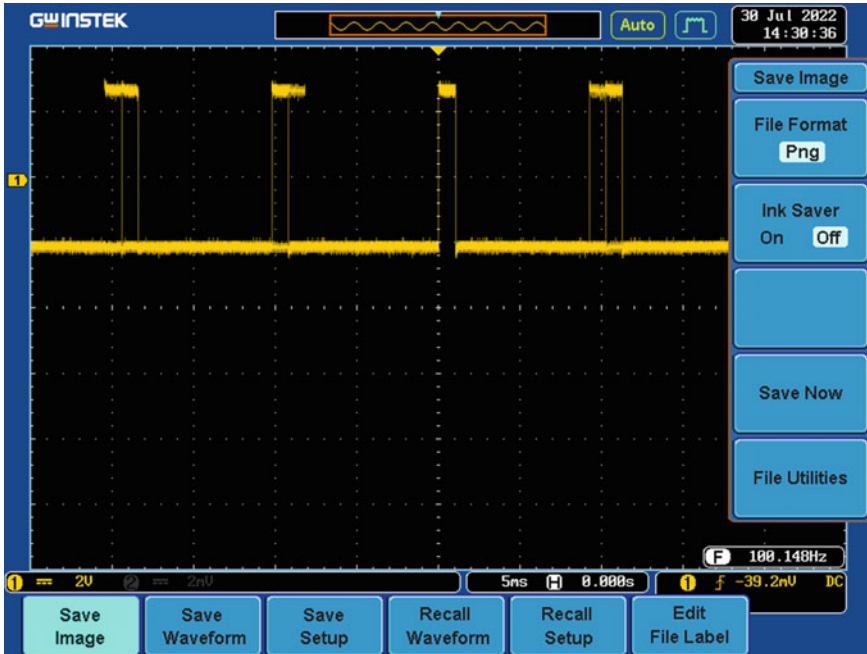


Fig. 7 Testing of sampling frequency on the oscilloscope digital

3.2 Research Results

Results of the Butterworth filter on the phantom

Figure 8 shows a graph of the mean dominant frequency yielded from the analysis using the FFT method on the phantom data with respiration rate settings of 15, 20, and 30 Brpm of the Butterworth filter in orders 4, 6, and 8.

Results of the Chebyshev I filter on the phantom

Figure 9 shows a graph of the mean dominant frequency yielded from the analysis using the FFT method on the phantom data with respiration rate settings of 15, 20, and 30 Brpm of the Chebyshev I filters in orders 4, 6, and 8.

The shape of Respiration Rate signal on the phantom

Figure 10a shows the shape of the ECG signal before filtering and Fig. 10b shows the shape of the Respiration Rate signal based on the extraction from the lead II ECG signal using the Butterworth filter in orders 4, 6, and 8.

Figure 11a shows the shape of the ECG signal before filtering and Fig. 11b shows the shape of the Respiration Rate signal based on extraction from the lead II ECG signal using the Chebyshev I filter in orders 4, 6, and 8.

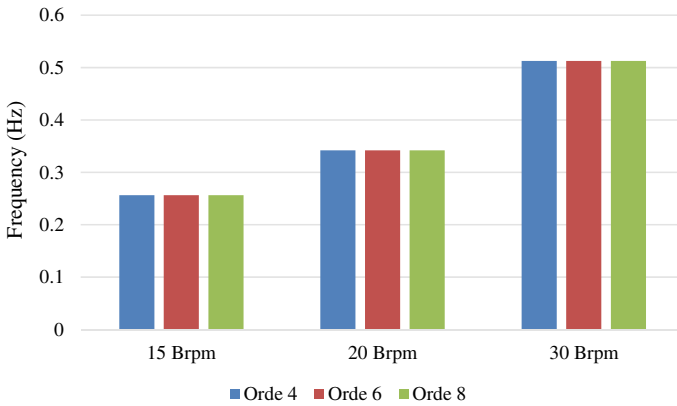


Fig. 8 Mean frequency FFT of the Butterworth filter on the phantom

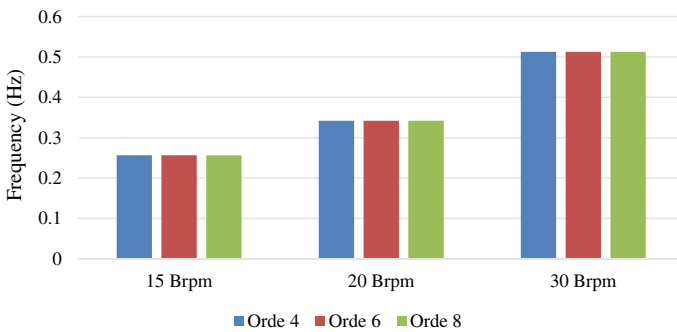


Fig. 9 Mean frequency FFT of the Chebyshev I filter on the phantom

Table 1 shows the results of the number of Respiration Rate signal, error values, standard deviations, and type values of the Butterworth and Chebyshev I filters in Order 4. Then, Table 2 shows the results of the number of Respiration Rate signal, error values, standard deviations, and type values of the Butterworth and Chebyshev I filters in Order 6. Finally, Table 3 shows the results of the number of Respiration Rate signal, error values, standard deviations, and type values of the Butterworth and Chebyshev I filters in Order 8.

Results of the Butterworth filter on respondents

Figure 12 shows a graph of the mean dominant frequency yielded from the analysis using the FFT method on Respondent data using the Butterworth filter in orders 4, 6, and 8.

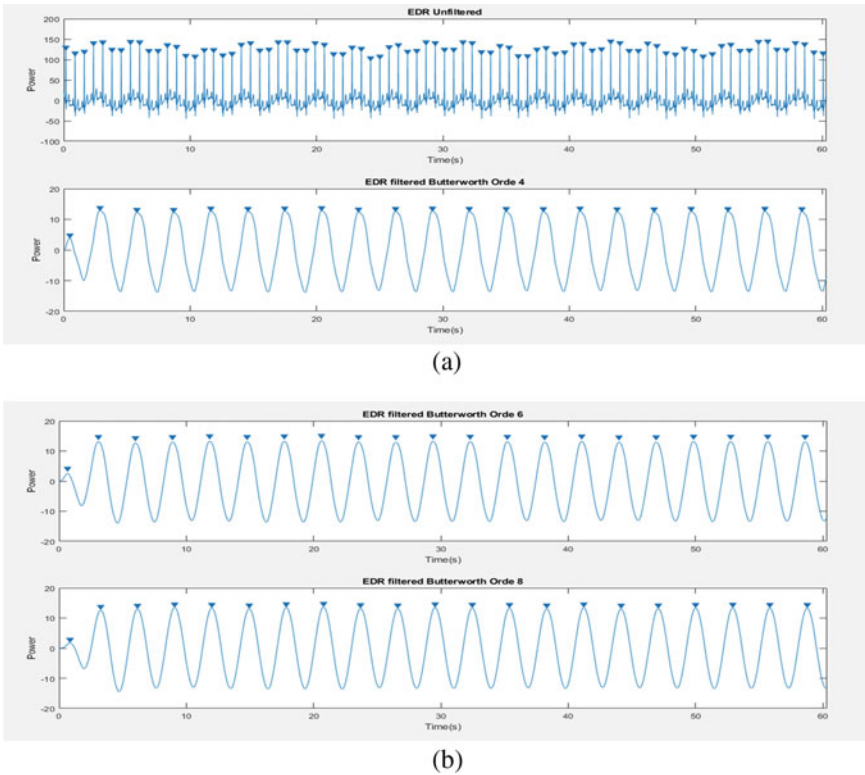


Fig. 10 a ECG signal. b Shape of the Butterworth filter signal on the phantom

Results of the Chebyshev I filter on respondents

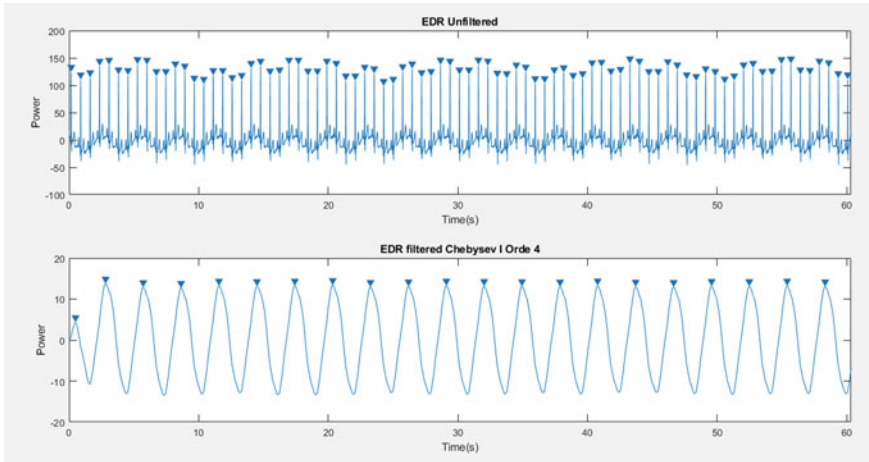
Figure 13 shows a graph of the mean dominant frequency yielded from the analysis using the FFT method on Respondent data using the Chebyshev I filter in orders 4, 6, and 8.

The shape of Respiration Rate signal on respondents

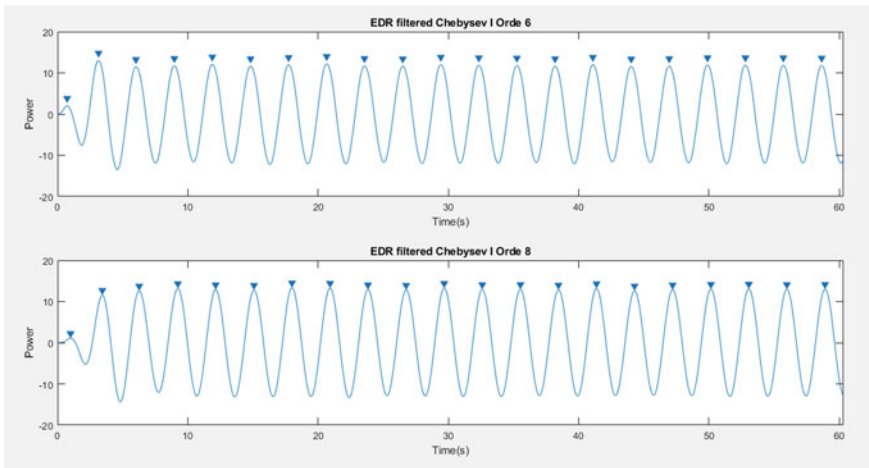
Figure 14a shows the shape of the ECG signal before filtering on Respondents and the filter result of order 4. Figure 11b shows the shape of Respiration Rate signal based on the extraction from the lead II ECG signal using the Butterworth filter in orders 4, 6, and 8.

Figure 15a shows the shape of the ECG signal before filtering on respondents and the filter result of order 4. Figure 15b shows the shape of Respiration Rate signal based on the extraction from the lead II ECG signal using the Chebyshev I filter in orders 6 and 8 (Fig. 15).

Table 4 shows the results of the number of Respiration Rate signal and error values of the Butterworth and Chebyshev I filter in each order. The data were obtained from the calculation of the peak count signal EDR. From the data, information was



(a)



(b)

Fig. 11 Shape of the Chebyshev I filter signal on the phantom

Table 1 Results of the respiration rate on the phantom in order 4

Phantom (BPM)	Order 4		Error	
	BF	CT1F	BF (%)	CT1F (%)
15	27.17	29.97	81.1	99.8
20	20.97	24.17	4.8	20.8
30	30.27	30.60	0.9	2.0
Mean	26.13	28.24	28.9	40.9

Table 2 Results of the respiration rate on the phantom in order 6

Phantom (BRPM)	Order 6		Error	
	BF	CT1F	BF (%)	CT1F (%)
15	15.73	15.63	4.89	4.22
20	20.57	20.33	2.83	1.67
30	30.33	30.23	1.11	0.78
Mean	22.21	22.07	2.94	2.22

Table 3 Results of the respiration rate on the phantom in order 8

Phantom (BRPM)	Order 8		Error	
	BF	CT1F	BF (%)	CT1F (%)
15	15.57	15.53	3.78	3.56
20	20.47	20.23	2.33	1.17
30	30.17	30.13	0.56	0.44
Mean	22.07	21.97	2.22	1.72

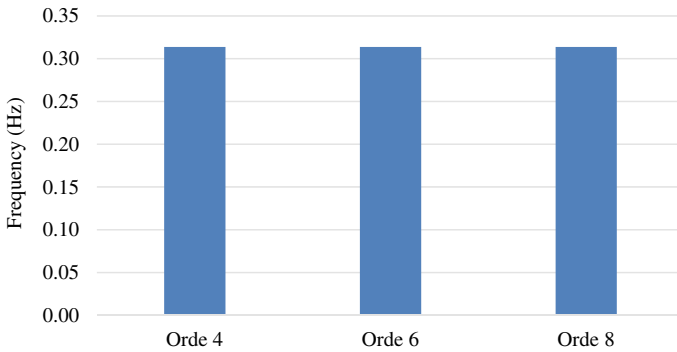


Fig. 12 Mean frequency FFT of the Butterworth filter on respondents

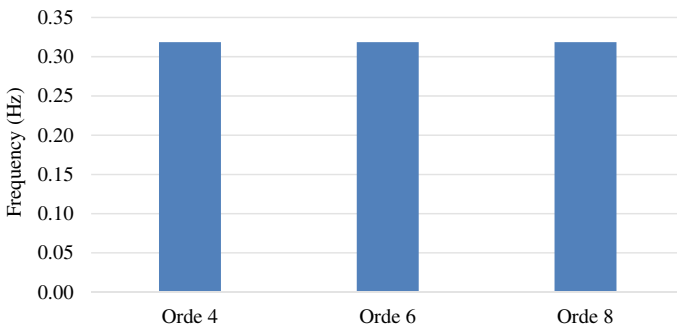
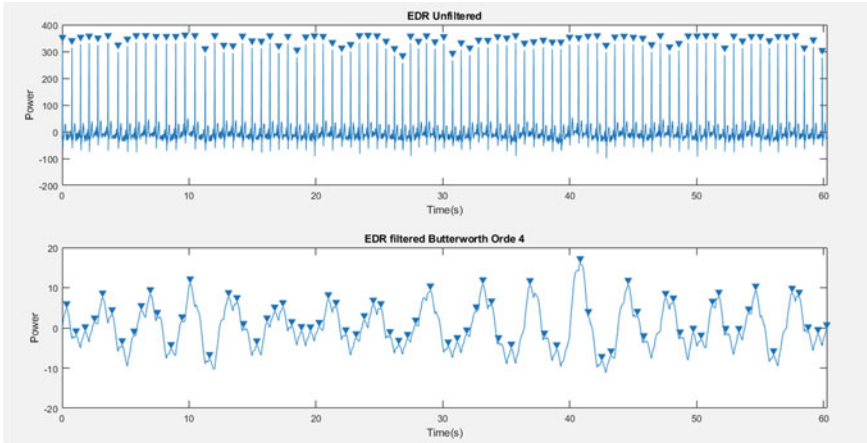
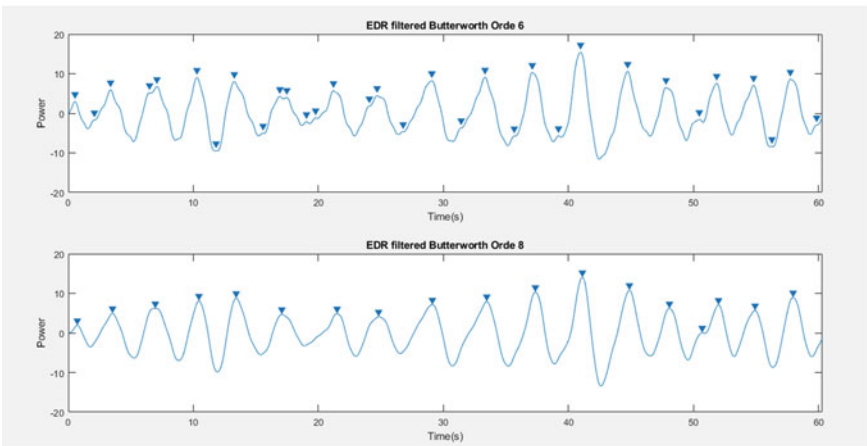


Fig. 13 Mean frequency FFT of the Chebyshev I filter on respondents



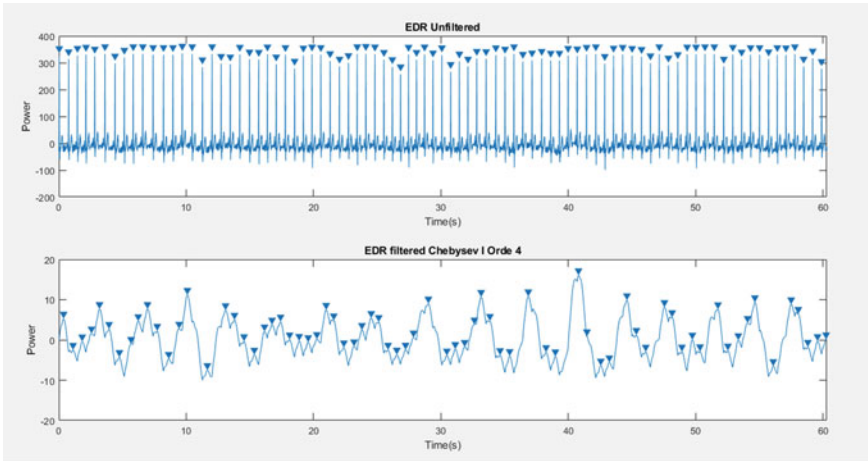
(a)



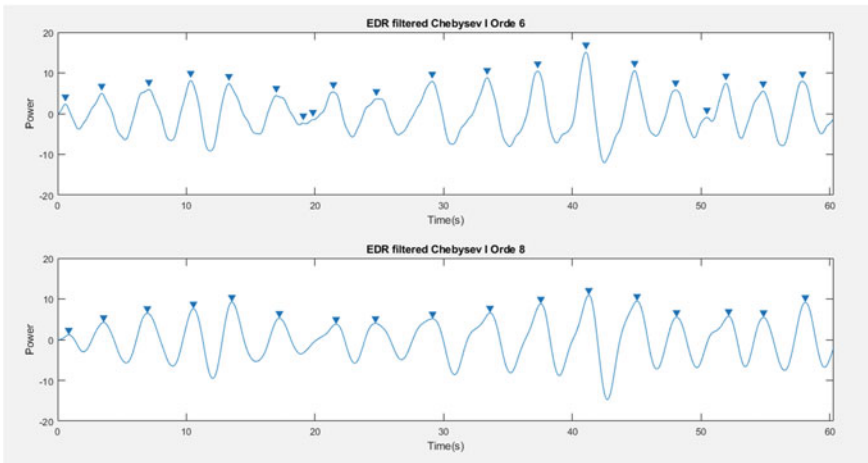
(b)

Fig. 14 a, b The shape of Butterworth filter signal on respondents

obtained that the smallest error value of the Chebyshev I filter in order 8 was 4%, and the largest error value was obtained in order 4. This is because in order 4, the resulting signal has a lot of noise so that the peak count has a large error value. This proves that the higher the order of the signal, the better the results, so the error of measuring the respiration rate using the peak count is smaller. Figure 16 shows the graph (boxplot) of the value of the respiration rate signal in respondents, and it can be seen from the graph that order 8 data distribution is more centralized from both the Butterworth and the Chebyshev I filter.



(a)



(b)

Fig. 15 a, b The shape of Chebyshev I filter signal on respondents

Table 4 Respiration rate error value on respondents

Order	Setting (BRPM)	Filter type		Error %	
		BF	CT1F	BF (%)	CT1F (%)
4	21.1	71.4	70.1	238.4	232.2
6		36.3	27.3	72.0	29.4
8		23	21.9	9.0	3.8

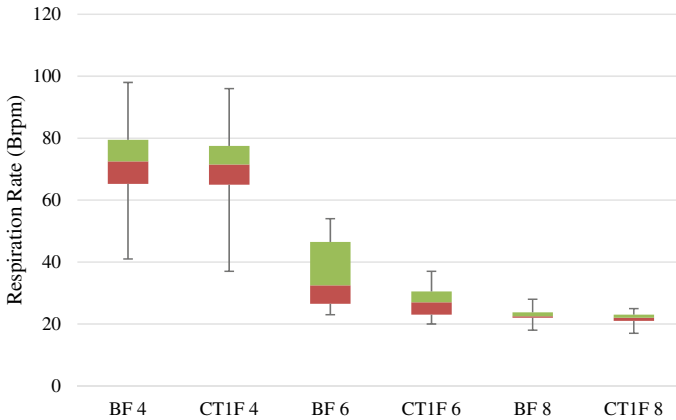


Fig. 16 Respiration rate error value on respondents

3.3 Correlation Analysis

The correlation value (r) ranges from 1 to -1 ; the value closer to 1 or -1 means that the relationship between the two variables is getting stronger, on the contrary the value closer to 0 means that the relationship between the two variables is getting weaker. A positive value indicates a unidirectional relationship (X goes up then Y goes up) and a negative value indicates an inverse relationship (X goes up then Y goes down). According to Sugiyono [34], the guidelines for providing interpretation of the correlation coefficient are 0.00–0.199 for very low, 0.20–0.399 for low, 0.40–0.599 for medium, 0.60–0.799 for strong and 0.80–1.000 for very strong.

Butterworth filter. The PSD components were yielded from the phantom and respondents signals using the Butterworth filter with different orders, namely orders 4, 6, and 8 with Respiration Rate settings of 15, 20, and 30 brpm and heart rate settings of 80, 90, and 100 bpm. Furthermore, the component values taken include Mean F , which is a table of mean frequency value, Mean P , which is a mean power value, and Median F , which is a middle value of frequencies. Then, the data were analyzed using a correlation analysis between the phantom values and respondent values. Table 7 shows the results of correlation between the phantom and respondents in orders 4, 6, and 8. Based on the results of the correlation analysis values for the phantom and respondents using the Butterworth filter, the highest (strongest) correlation value is 0.996982309 in order 6.

Chebyshev, I filter. The PSD components were yielded from the phantom and respondent signals using the Chebyshev I filter with different orders, namely orders 4, 6, and 8 with Respiration Rate settings of 15, 20, and 30 brpm and heart rate settings of 80, 90, and 100 bpm in Orders 4, 6 and 8. Furthermore, the component values taken include Mean F , which is a table of mean frequency values, Mean P , which is a mean power value, and Median F , which is a middle value of frequencies. Then, the data were analyzed using a correlation analysis between the phantom values and

respondent values. Table 8 shows the results of correlation between the phantom and respondents in orders 4, 6, and 8. Based on the results of the correlation analysis values for the phantom and respondents using the Chebyshev I filter, the highest (strongest) correlation is 0.999669555 in order 8.

4 Discussion

Figures 8 and 9 show graphs of the mean dominant frequency yielded from the FFT method after using the Butterworth and Chebyshev I filters with a respiration rate of 15 Brpm on the phantom, showing the same result of 0.2563 Hz in each order. Furthermore, a respiration rate of 20 Brpm on the phantom showed a result of 0.3418 Hz in each order. Then, a respiration rate of 30 Brpm on the phantom also showed the same result of 0.5127 Hz in each order. Figure 12 shows a graph of the mean dominant frequency of the respiration rate signal yielded from the FFT method after using the Butterworth filter on respondents, showing the same result of 0.31 Hz and Fig. 13 shows a graph of the mean dominant frequency of the respiration rate signal yielded from the FFT method after using the Chebyshev I filter on respondents, showing the same result of 0.32 Hz in each order. In the Butterworth and Chebyshev, which I filter in each order, both from the phantom and respondents' data, it is shown the frequency value of the respiration rate signal that had been extracted from the ECG signal, namely the frequency range of 0.1–0.5 Hz.

Tables 1, 2, and 3 show the results on MATLAB processing based on the phantom data in the form of a Respiration Rate signal extracted from an ECG signal, showing the smallest error value in the Chebyshev I (CT1F) filter in order 8 of 1.72%. Then Tables 4, 5, and 6 show the results on MATLAB processing based on respondents' data in the form of a Respiration Rate signal extracted from the ECG signal, showing the smallest error value in the Chebyshev I (CT1F) filter in order 8 of 3.8%. It can be concluded that the extraction results of the Respiration Rate signal based on the ECG signal with the Butterworth and Chebyshev I filter in orders 4, 6, and 8, the best result was found in the Chebyshev I (CT1F) filter in order 8 from both the phantom and respondents' data.

The correlation between the phantom and respondents with Mean *F*, Mean *P*, and Median *F* components in the Butterworth filter, namely in Table 7, showed the highest (strongest) correlation result, namely in order 6 of 0.996982309. Meanwhile,

Table 5 Correlation coefficient in the Butterworth filter

Correlation between the phantom and respondents	Correlation coefficient	Correlation category
Order 4	0.568053032	Medium
Order 6	0.996982309	Very strong
Order 8	0.415058226	Medium

Table 6 Correlation coefficient in the Chebyshev I filter

Correlation phantom and respondents	Correlation coefficient	Correlation category
Order 4	0.95936178	Very strong
Order 6	0.99858902	Very strong
Order 8	0.999669555	Very strong

the correlation between the phantom and respondents with Mean F , Mean P , and Median F components in the Chebyshev I filter, namely in Table 8, showed the highest (strongest) correlation result, namely in in order 8 of 0.999669555. This suggests that the Chebyshev I filter of order 8 is better than the Butterworth filter because the correlation value obtained reaches 0.999.

The results of this correlation are positive results (positive correlations), which means the correlation between the two variables, in this case are the phantom and respondents, is in the same direction. That is, if variable X increases then variable Y also increases or vice versa. It can be concluded that the correlation value is very strong. It can prove the effectiveness in extracting the Respiration Rate signal based on the ECG signal, namely the Chebyshev I filter in order 8.

When compared to the previous studies [20, 21], this study has succeeded in comparing the effectiveness of the use of IIR digital filters with an increase in orders where the most effective filter to extract respiration rate signal from ECG signal was obtained, namely the Chebyshev I filter of order 8. This is shown from the results of the error value of the respiration signal from a gold standard and respondents which are smaller than the previous studies [4].

5 Conclusion

This study was conducted to determine the effectiveness of the use of the Infinite Impulse Response (IIR) digital filter in the design of the Butterworth Filter and the Chebyshev I filter with an increase in orders 4, 6, and 8 in extracting the respiration rate signal based on the ECG signal. The results of this study showed that the Chebyshev I filter of order 8 was better than the Butterworth filter based on the analysis of the highest (strongest) correlation from the phantom to respondents, and based on the smallest error values of both the phantom and respondents' respiration rate signals.

The disadvantage of the research that has been carried out is that, it has not been able to calculate the Respiration Rate in real time and there is no display in the form of a signal processing software on MATLAB. It is hoped that this study can add insight and knowledge about the Respiration Rate Signal extraction Method, especially using the digital filters on MATLAB, and can be used as a reference for subsequent studies.

References

1. Jagadev P, Giri LI (2020) Non-contact monitoring of human respiration using infrared thermography and machine learning. *Infrared Phys Technol* 104:103117. <https://doi.org/10.1016/j.infrared.2019.103117>
2. Charlton PH, Bonnici T, Tarassenko L, Clifton DA, Beale R, Watkinson PJ (2016) An assessment of algorithms to estimate respiratory rate from the electrocardiogram and photoplethysmogram. *Physiol Meas* 37:610–626. <https://doi.org/10.1088/0967-3334/37/4/610>
3. Miyagi SA, Mak'ruf MR, Setioningsih ED, Das T (2020) Design of respiration rate meter using flexible sensor. *J Electron Electromed Eng Med Inform* 2:13–18. <https://doi.org/10.35882/jee.emi.v2i1.3>
4. Orphanidou C (2017) Derivation of respiration rate from ambulatory ECG and PPG using ensemble empirical mode decomposition: comparison and fusion. *Comput Biol Med* 81:45–54. <https://doi.org/10.1016/j.compbiomed.2016.12.005>
5. Sarotama A (2019) Melyana: Implementasi Peringatan Abnormalitas Tanda-Tanda Vital pada Telemedicine Workstation. *J Nas Sains dan Teknol* 21:1–9
6. Bao X, Howard M, Niazi IK, Nlandu Kamavuako E (2020) Comparison between embroidered and gel electrodes on ECG-derived respiration rate. In: *Proceedings of the annual international conference of the IEEE engineering in medicine and biology society EMBS, 2020 July*, pp 2622–2625. <https://doi.org/10.1109/EMBC44109.2020.9176485>
7. Maghfiroh AM, Arifin A, Sardjono TA (2019) Wavelet-based respiratory rate estimation using electrocardiogram. In: *Proceedings of the 2019 international seminar on intelligent technology and its applications ISITIA 2019*, pp 354–359. <https://doi.org/10.1109/ISITIA.2019.8937201>
8. Lázaro J, Reljin N, Bailón R, Gil E, Noh Y, Laguna P, Chon KH, Member S (2020) Electrocardiogram derived respiratory rate using a wearable armband. *IEEE Trans Biomed Eng* 9294. <https://doi.org/10.1109/TBME.2020.3004730>
9. Sarkar S, Bhattacharjee S, Pal S (2015) Extraction of respiration signal from ECG for respiratory rate estimation. *IET Conf Publ* 2015:336–340. <https://doi.org/10.1049/cp.2015.1654>
10. Varon C, Morales J, Lázaro J, Orini M, Deviaene M, Kontaxis S, Testelmans D, Buyse B, Borzée P, Sörnmo L, Laguna P, Gil E, Bailón R (2020) A comparative study of ECG-derived respiration in ambulatory monitoring using the single-lead ECG. *Sci Rep* 10:1–14. <https://doi.org/10.1038/s41598-020-62624-5>
11. Pimentel MAF, Charlton PH, Clifton DA (2015) Probabilistic estimation of respiratory rate from wearable sensors. *Smart Sensors Meas Instrum* 15:241–262. https://doi.org/10.1007/978-3-319-18191-2_10
12. Otrokov MM, Klimovskikh II, Calleja F, Vilkov O, Rybkin AG, Estyunin D, Mu S, Vázquez de Parga AL, Miranda R, Guinea F, Cerdá JI, Chulkov EV (2018) Extraction of respiratory signals from the electrocardiogram and photoplethysmogram: technical and physiological determinants. 0–13
13. Raquel G, Laguna P (2013) Deriving respiration from photoplethysmographic pulse width. 233–242. <https://doi.org/10.1007/s11517-012-0954-0>
14. Charlton PH, Villarroel M, Salguero F (2016) Waveform analysis to estimate respiratory rate. *Second Anal Electron Heal Rec* 377–390. <https://doi.org/10.1007/978-3-319-43742-2>
15. Jan HY, Chen MF, Fu TC, Lin WC, Tsai CL, Lin KP (2019) Evaluation of coherence between ECG and PPG derived parameters on heart rate variability and respiration in healthy volunteers with/without controlled breathing. *J Med Biol Eng* 39:783–795. <https://doi.org/10.1007/s40846-019-00468-9>
16. Sarkar S, Bhattacharjee S, Pal S (2015) Extraction of respiration signal from. *Michael Faraday IET Int Summit* 336–340
17. Sharma H, Sharma KK, Bhagat OL (2015) Respiratory rate extraction from single-lead ECG using homomorphic filtering. *Comput Biol Med* 59:80–86. <https://doi.org/10.1016/j.compbiomed.2015.01.024>
18. Basu S (2020) Comparative study on the effect of order and cut off frequency of Butterworth low pass filter for removal of noise in ECG signal. *IEEE Int Conf Converg Eng* 156–160

19. Leonard C, Sabrina NH, Bayuntara PGA, Ariel Y (2020) Analisis Keefektifan Penggunaan Filter FIR dan IIR pada Sinyal Pernapasan EMGdi dengan Simulasi MATLAB. *Ultim Comput XII*
20. Sharma H, Sharma KK, Bhagat OL (2015) Respiratory rate extraction from single-lead ECG using homomorphic filtering. *Comput Biol Med (Elsevier)* 59:80–86. <https://doi.org/10.1016/j.combiomed.2015.01.024>
21. Jagadev P, Giri LI (2020) Non-contact monitoring of human respiration using infrared thermography and machine learning. *Infrared Phys Technol (Elsevier)* 104:103117. <https://doi.org/10.1016/j.infrared.2019.103117>
22. Zhuang S, Li F, Zhuang Z, Rao W, Joseph Raj AN, Rajangam V (2021) Improved ECG-derived respiration using empirical wavelet transform and Kernel principal component analysis. *Comput Intell Neurosci*. <https://doi.org/10.1155/2021/1360414>
23. Sohr-t-petersen L (2014) Evaluation of algorithms for ECG derived respiration in the context of heart rate variability studies. 1–77
24. Rahman AM (2018) A comparison of three ECG-derived respiration methods for sleep apnoea detection. *Biomed Phys Eng Express* 0–68
25. Lenis G, Conz F, Dössel O (2015) Combining different ECG derived respiration tracking methods to create an optimal reconstruction of the breathing pattern. *Curr Dir Biomed Eng* 1:54–57. <https://doi.org/10.1515/cdbme-2015-0014>
26. Gargiulo GD, Bifulco P, Cesarelli M, McEwan AL, Moeinzadeh H, O’loughlin A, Shugman IM, Tapson JC, Thiagalingam A (2018) On the einthoven triangle: a critical analysis of the single rotating dipole hypothesis. *Sensors (Switzerland)* 18. <https://doi.org/10.3390/s18072353>
27. Kusuma DT (2020) Fast Fourier Transform (FFT) Dalam Transformasi Sinyal Frekuensi Suara Sebagai Upaya Perolehan Average Energy (AE) Musik. *Petir* 14:28–35. <https://doi.org/10.33322/petir.v14i1.1022>
28. Francis J (2016) ECG monitoring leads and special leads. *Indian Pacing Electrophysiol J* 16:92–95. <https://doi.org/10.1016/j.ipej.2016.07.003>
29. Drew BJ, Califf RM, Funk M, Kaufman ES, Krucoff MW, Laks MM, Macfarlane PW, Sommargren C, Swiryn S, Van Hare GF (2004) Practice standards for electrocardiographic monitoring in hospital settings: an American Heart Association scientific statement from the councils on cardiovascular nursing, clinical cardiology, and cardiovascular disease in the young. *Circulation* 110:2721–2746. <https://doi.org/10.1161/01.CIR.0000145144.56673.59>
30. Lidyawati L, Darlis AR, Tamba AF (2016) Implementasi Filter Infinite Impulse Response (Iir) Dengan Respon Butterworth Dan Chebyshev Menggunakan Dsk Tms320C6713. *J Elektro dan Telekomun Terap* 2:95–103. <https://doi.org/10.25124/jett.v2i1.97>
31. Sidney Burrus C, Frigo M, Johnson SG, Markus Puschel IS (2012) Fast Fourier transforms. Texas
32. Lubis MZ, Batam PN, Manik H (2016) Signal processing for power spectral density. <https://doi.org/10.13140/RG.2.1.2106.2006>
33. CCA. Analog to digital converter module of ATmega328P
34. Sugiyono (2014) Metode Penelitian kuantitatif, kualitatif dan R & D. Alfabeta, Bandung